Article

pubs.acs.org/Biomac

Cationic Spacer Arm Design Strategy for Control of Antimicrobial Activity and Conformation of Amphiphilic Methacrylate Random Copolymers

Edmund F. Palermo,[†] Satyavani Vemparala,*[,§] and Kenichi Kuroda*[,†,‡]

[†]Macromolecular Science and Engineering Center and [‡]Department of Biologic and Materials Sciences, School of Dentistry, University of Michigan, Ann Arbor, Michigan 48109, United States

[§]The Institute of Mathematical Sciences, CIT Campus, Taramani, Chennai 600113, India

Supporting Information

ABSTRACT: Antimicrobial and hemolytic activities of amphiphilic random copolymers were modulated by the structure of the cationic side chain spacer arms, including 2-aminoethylene, 4-aminobutylene, and 6-aminohexylene groups. Cationic amphiphilic random copolymers with ethyl methacrylate (EMA) comonomer were prepared with a range of comonomer fractions, and the library of copolymers was screened for antimicrobial and hemolytic activities. Copolymers with 4-aminobutylene cationic side chains showed an order of magnitude enhancement in their antimicrobial activity relative to those with 2-aminoethylene spacer arms, without causing adverse hemolysis. When the spacer arms were further elongated to hexylene, the copolymers displayed potent antimicrobial and hemolytic activities. The 4-aminobutylene side chain appears to be the optimal spacer arm length for maximal antimicrobial potency and minimal hemolysis, when combined with hydrophobic ethylmethacrylate in a roughly 70/30 ratio. The copolymers displayed relatively rapid bactericidal kinetics and broad-spectrum activity against a panel of Gram-positive and Gram-negative bacteria. The effect of the spacer arms on the polymer conformation in the membrane-bound state was investigated by molecular dynamics simulations. The polymer backbones adopt an extended chain conformation, parallel to the membrane surface. A facially amphiphilic conformation at the membrane surface was observed, with the primary ammonium groups localized at the lipid phoshophate region and the nonpolar side chains of EMA comonomers buried in the hydrophobic membrane environment. This study demonstrates that the antimicrobial activity and molecular conformation of amphiphilic methacrylate random copolymers can be modulated by adjustment of cationic side chain spacer arms.

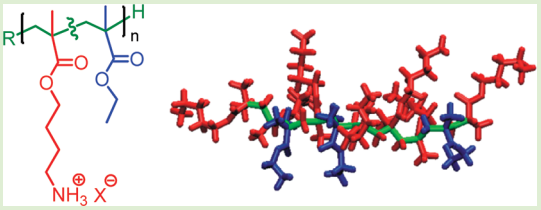

INTRODUCTION

With the rapid spread of antibiotic-resistant bacterial infections, coupled to a decline in the availability of new antibiotic drugs, there is now an urgent need for compounds that exert novel mechanisms of antimicrobial action.[1] In nature, the release of host defense antimicrobial peptides (AMPs) by eukaryotes is a key component of innate immunity to invasion by pathogenic bacteria because AMPs are able to kill a broad spectrum of bacteria, without harming host cells and with a lower likelihood of inducing resistance.[2] Hence, there is substantial interest in utilizing them to combat infectious diseases, and many peptide antibiotics are currently in clinical trials.[3] The mechanisms of AMP action are complex and diverse: the peptides have been shown to permeabilize bacterial cell membranes, inhibit intracellular targets to cause direct killing of the invading pathogens, and modulate the host immune system.[4−6] Recent transcriptional analyses have revealed that certain AMPs induce responses in the bacteria as a result of subinhibitory challenges.[7,8] Of these known effects, the membrane-disrupting ability of the peptides has attracted much attention, particularly in the field of synthetic polymer mimics.[9] Because the membrane disruption event is modulated by physiochemical parameters such as charge and amphiphilicity, the membrane-targeting antimicrobial function of AMPs has been successfully emulated by synthetic peptides[10] and peptoids[11] that exert antimicrobial activity with low toxicity to human cells. The central goal of this biomimetic approach is to capture the physiochemical features of the naturally occurring peptides rather than reproducing the exact chemical structures. In that light, Tew and DeGrado developed cationic, amphiphilic arylamide oligomers, which are currently in clinical trials as antibiotic drugs.[12,13] Further mimicry of AMPs has encompassed amphiphilic homopolymers[14] and random copolymers[15,16] that exert antimicrobial activity with minimal toxicity after extensive optimization of their structural characteristics.

Membrane disruption is chiefly modulated by the molecular weight (MW), cationic charge, and amphiphilicity of the peptides.[5,17,18] Cationic groups are initially attracted to the anionic components of bacterial membranes.[19] Membrane binding induces secondary structure in which the cationic and

Received: March 2, 2012
Revised: April 3, 2012
Published: April 5, 2012

hydrophobic side chains of amino acid residues are segregated to opposing domains, known as "facially amphiphilic" structures.[20] The facially amphiphilic structure of these peptides is believed to be a key factor in their potent antimicrobial activity as well as selective toxicity to bacterial cells over host cells. As such, compounds that can adopt facially amphiphilic conformation show substantial promise as peptide-mimics such as β-peptides[21,22] and peptoids.[11] A wide variety of synthetic amphiphilic random copolymers based on methacrylates,[23] methacrylamides,[24] norbornenes,[14] and nylon-3 derivatives[25] have been designed to mimic the physiochemical features and functions of AMPs. These polymers have been shown to inhibit bacterial growth with minimal harm to human red blood cells (RBCs). These random copolymers are not designed to have intrinsic facially amphiphilic secondary conformations. However, they may be capable of adopting irregular but facially amphiphilic confirmations on the cell membrane given sufficient backbone flexibility.[16] Such a hypothesis has been previously proposed by Gellman and coworkers regarding their antimicrobial nylon-3 copolymers.[25] We have demonstrated that the ammonium groups of methacrylate copolymers are likely to form a complex with phosphate lipid head groups by a combination of electrostatic and hydrogen bonding effects, which enhance the affinity of polymers for lipid membranes.[26] Sum frequency generation (SFG) spectroscopy showed that the hydrophobic side chains in the same copolymers interact with the nonpolar lipid alkyl tails.[27] This experimental evidence suggests that the ammonium groups of the copolymers interact with phosphate lipid head groups while the hydrophobic side chains of comonomers are inserted into the membranes. Accordingly, it is possible for the flexible polymethacrylae chains to adopt facially amphiphilic conformation in the membrane, despite their lack of defined monomer sequence and intrinsic secondary structures.

One of the key parameters that has not been systematically studied is the chemical identity and length of cationic spacer arms in the side chains of copolymers, likely to affect the amphiphilic properties of polymers. The variation of spacer arms may also affect the conformation of polymers and insertion into cell membranes: a related concept is the snorkeling effect for peptides with long ammonium side-chain spacer arms, in which the ammonium spacer arms reach to the water−lipid interface, allowing nonpolar peptide helices to localize in the hydrophobic domains of lipid bilayers.[28,29] The position and orientation of hydrophobic transmembrane helices can be modulated by the snorkel effect. Insertion of transmembrane helices, possessing mismatch between peptide length and the thickness of hydrophobic core in a lipid bilayer, was facilitated by electrostatic interaction between lipid phosphate groups and lysine segment at either helix end.[30] Similarly, snorkeling of an arginine residue at the helix end reduces the energy for insertion of helices, allowing transmembrane configuration.[31] The position of transmembrane helices in lipid bilayers was also controlled by incorporation of lysine or arginine in the middle of sequence, which snorkels toward the lipid−water interface.[32]

In the case of heterogeneous synthetic polymers, longer alkyl spacer arms may facilitate membrane insertion by analogy to the snorkel effect. These putative effects of spacer arms on the polymer properties and conformations in lipid bilayers could furthermore modulate their antibacterial activity. Recently, adjustment of spacer arms has also been utilized for tuning the activity of cell-penetrating peptoids, which showed improved cell uptake as the spacer lengths were increased.[33] However, this design concept has never been applied to antimicrobial polymers to the best of our knowledge. The advantage of such a design approach is that the spacer group parameter can be tuned for controlling the antimicrobial activity without changing the ratio of the number of cationic ammonium groups to hydrophobic comonomers.

To that end, we demonstrate the role played by the spacer groups in terms of antimicrobial and hemolytic activities. The cationic spacer arms have various lengths and structures (ethylene, butylene, hexylene, and cyclohexylene) to assess their effects on the activities systematically. Furthermore, we employed molecular dynamics simulations to investigate the conformations of the copolymers when bound to anionic lipid bilayers.

MATERIALS AND METHODS

Materials. 2,2′-Azobisisobutyronitrile (AIBN) was purchased from Sigma-Aldrich, and ethyl methacrylate (EMA), methyl 3-mercaptopropionate (MMP), ethanolamine, 4-butanolamine, 6-hexanolamine, and di-*tert*-butyldicarbonate were purchased from Acros and used without further purification. Methacryloyl chloride was purchased from Acros and was freshly distilled prior to each use. Trifluoroacetic acid and reagent grade solvents were purchased from Fisher, and the bee venom toxin melittin (>85%) was purchased from Sigma. Gel permeation chromatography (GPC) was performed using a Waters 1515 pump and RI detector. Gas chromatography was performed on a Shimadzu GC-2010. Human RBCs (leukocytes reduced adenine saline added) were obtained from the American Red Cross Blood Services Southeastern Michigan Region and used prior to the out date indicated on each unit. The bacteria were obtained from ATCC: *Escherichia coli* (ATCC 25922), *Staphylococcus aureus* (ATCC 25923), *Enterococcus faecalis* (ATCC 29212), *Bacillus subtilis* (ATCC 6633), *Acinetobacter baumannii* (ATCC 17978), *Pseudomonas aeruginosa* (ATCC 27853), and *Salmonella enterica* (ATCC 14028). MRSA LAC 1263 was provided by Dr. Boles at the University of Michigan.

Monomer Synthesis. To a solution of ethanolamine (42.7 mmol, 2.6 g) in a biphasic mixture of THF (30 mL) and NaOH(aq) (1 M, 50 mL) was added a solution of di-*tert*-butyldicarbonate (42.7 mmol, 9.3 g) in THF (20 mL) dropwise, and the mixture was stirred at room temperature overnight. The resulting *N*-Boc-protected alcohol was extracted in ethylacetate by washing with water, saturated $NaCO_3H$-(aq), and brine. The same procedure was followed in the case of 4-butanolamine, 6-hexanolamine, and *trans*-4-aminocyclohexanol. Freshly distilled methacryloyl chloride (23 mmol, 2.2 mL) was diluted with dichloromethane (5 mL) and added dropwise to a solution of the *N*-Boc-protected alcohol (23 mmol) and triethylamine (25 mmol, 3.5 mL) in dichloromethane (50 mL) at 0 °C ice bath, and the mixture was allowed to stir overnight. The solution was then filtered, and the filtrate was concentrated under reduced pressure, extracted in ethylacetate by washing with water, saturated $NaCO_3H$(aq), and brine. Figure 1 shows the monomers **1**−**4** prepared in this work.

The monomer 2-(*tert*-butoxycarbonylamino)ethyl methacrylate, **1**, was recrystallized from hexanes at −20 °C to give a white solid in 72% yield. ^{1}H NMR (400 MHz, $CDCl_3$): δ 6.09 (s, 1H), 5.55 (s, 1H), 4.73 (bs), 4.17 (t, 2H), 3.40 (q, 2H), 1.91 (s, 3H), 1.41 (s, 9H). ^{13}C NMR (100 MHz, $CDCl_3$): δ 167.27, 156.04, 136.00, 125.89, 79.56, 63.94, 39.67, 28.32, 18.27. Mass spectrometry: ESI calcd for $[C_{11}H_{19}NO_4 + Na]^+$, 252.1212; found, 252.1209.

The monomer 4-(*tert*-butoxycarbonylamino)butyl methacrylate, **2**, was purified by silica gel column chromatography (eluent: hexane/ethyl acetate 3:1) to give a colorless, viscous oil in 81% yield. Thin layer chromatography (eluent: hexane/ethyl acetate 3:1) R_f = 0.54, I_2 stained. ^{1}H NMR (300 MHz, $CDCl_3$): δ 6.09 (s, 1H), 5.55 (s, 1H), 4.54 (bs), 4.15 (t, 2H), 3.15 (q, 2H), 1.93 (s, 3H), 1.8−1.5 (m, 4H), 1.43 (s, 9H). ^{13}C NMR (100 MHz, $CDCl_3$): δ 167.35, 155.92, 136.34, 125.73, 79.16, 64.25, 40.11, 28.26, 26.73, 25.97, 18.21. Mass

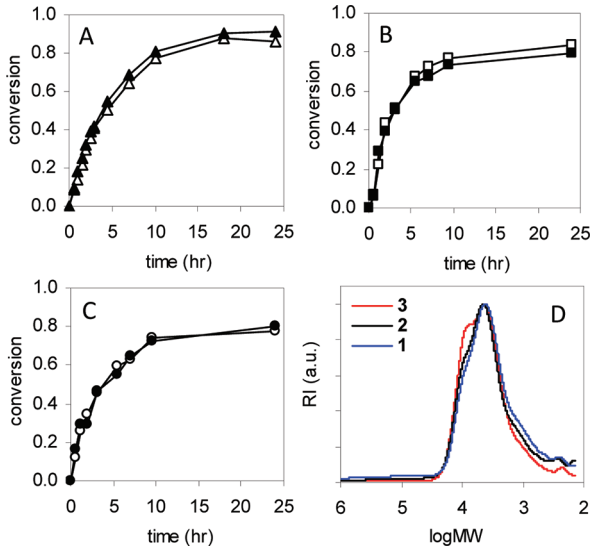

Figure 1. Conversion–time plots for the copolymerization of EMA with Boc-protected aminoalkylmethacrylates (A) **1**, (B) **2**, and (C) **3**. The monomer ratio of EMA to Boc-protected aminoalkylmethacrylates is 1:1. Gel-permeation chromatographs for each of the obtained copolymers, in THF relative to PMMA standards. M_n values are 4.9, 5.2, and 5.9 kDa, and PDI values are 1.52, 1.55, and 1.64 for the copolymers containing EMA and **1**, **2**, and **3**, respectively.

spectrometry: ESI calcd for $[C_{13}H_{23}NO_4 + Na]^+$, 280.1525; found, 280.1529.

The monomer 6-(*tert*-butoxycarbonylamino)hexyl methacrylate, **3**, was purified by silica gel column chromatography (eluent: hexane/ethyl acetate 9:1) to give a colorless, viscous oil in 68% yield. Thin layer chromatography (eluent: hexane/ethyl acetate 9:1) R_f = 0.90, I_2 stained. ^{1}H NMR (300 MHz, $CDCl_3$): δ 6.09 (s, 1H), 5.54 (s, 1H), 4.52 (bs), 4.13 (t, 2H), 3.10 (q, 2H), 1.93 (s, 3H), 1.67 (m, 2H), 1.5–1.3 (m, 6H), 1.43 (s, 9H). ^{13}C NMR (100 MHz, $CDCl_3$): δ 167.49, 155.95, 136.46, 125.19, 79.03, 64.58, 40.45, 29.96, 28.52, 28.39, 26.41, 26.67, 18.30. Mass spectrometry: ESI calcd for $[C_{15}H_{27}NO_4 + Na]^+$, 308.1838; found, 308.1833.

The monomer *trans*-4-(*tert*-butoxycarbonylamino)cyclohexyl methacrylate, **4**, was purified by recrystallization from ethyl acetate at −20 °C to give a white solid in 77% yield. Thin layer chromatography (eluent: hexane/ethyl acetate 9:1) R_f = 0.41, I_2 stained. ^{1}H NMR (300 MHz, $CDCl_3$): δ 6.08 (s, 1H), 5.54 (s, 1H), 4.74 (tt, 1H), 4.40 (bs), 3.47 (m, 1H), 2.02 (m, 4H), 1.92 (s, 3H), 1.6–1.4 (m, 2H), 1.44 (s, 9H), 1.35–1.15 (m, 2H). ^{13}C NMR (100 MHz, $CDCl_3$): δ 166.88, 155.20, 136.63, 125.21, 79.26, 72.05, 48.46, 30.73, 29.87, 28.37, 18.27. Mass spectrometry: ESI calcd for $[C_{15}H_{25}NO_4 + Na]^+$, 306.1681; found, 306.1681.

Polymer Synthesis. Random copolymers were prepared by a previously described technique[23] with minor alterations. EMA or butyl methacrylate (BMA) was dissolved with N-Boc-protected aminoalkyl methacrylate **1**, **2**, **3**, or **4** (1 mmol total monomers, various ratios) in acetonitrile (0.5 mL). AIBN (0.01 mmol) and MMP (0.1 mmol) were added from concentrated stock solutions. The mixtures were deoxygenated by nitrogen flushing for 2 min each and then submerged in a 70 °C oil bath overnight. After concentration under reduced pressure, the Boc-protecting groups were cleaved using trifluoroacetic acid and precipitated from methanol (0.5 mL) into diethyl ether (25 mL) twice. Obtained precipitates were lyophilized to afford the random copolymers as fine white powders.

Table 1. Characterization and Biological Activity Data for the Library of Copolymers and Peptides[a]

				MIC (μg/mL)[b]			HC_{50}/MIC	
	f_{HB}[c]	HDP[c]	M_n (kDa)[c]	*E. coli*	*S. aureus*	HC_{50} (μg/mL)[d]	*E. coli*	*S. aureus*
Homopolymers (f_{HB} = 0)								
$E2_0$	0	12.3	3.1	2000	100	>2000	>1.0	>20
$E4_0$	0	10.6	3.0	2000	250	>2000	>1.0	>8.0
$E6_0$	0	11.0	3.4	10	7.8	2.6	0.26	0.33
$Ec6_0$	0	10.1	3.1	1300	210	>2000	>1.5	>9.5
$B2_0$	0	15.3	3.9	1000	63	>2000	>2.0	>32
Copolymers (f_{HB} = 0.2 to 0.3)								
$E2_{28}$	0.28	13.5	2.9	250	125	>2000	>8.0	>16
$E4_{29}$	0.29	12.5	2.9	21	63	1300	62	21
$E6_{27}$	0.27	12.6	3.3	7.8	7.8	2.8	0.36	0.36
$Ec6_{28}$	0.28	11.5	2.9	21	31	860	41	28
$B2_{26}$	0.26	13.6	3.1	16	16	34	2.1	2.1
Copolymers (f_{HB} = 0.4 to 0.5)								
$E2_{45}$	0.45	16.2	3.1	13	42	76	5.8	1.8
$E4_{46}$	0.46	17.6	3.6	10	21	53	5.3	2.5
$E6_{40}$	0.40	14.5	3.4	6.5	10	2.3	0.35	0.23
$Ec6_{44}$	0.44	12.7	2.9	7.8	21	29	3.7	1.4
$B2_{40}$	0.40	19.6	4.1	16	16	9.0	0.56	0.56
Peptides								
magainin-2			2.5	125	>250	>250	>2	
melittin			2.8	12	5.6	1.7	0.14	0.30

[a]Comprehensive biological activity data for the entire library of copolymers in this work is given in the Supporting Information (Table S1). [b]Minimum inhibitory concentration (MIC), the concentration of polymer which completely inhibited growth of the bacteria after incubation in MH broth for 18 h at 37 °C. The initial challenge was ~5 × 10^5 cfu/mL. The data are rounded to two significant digits. [c]Mole fraction of hydrophobic repeat units EMA or BMA (f_{HB}), the average degree of polymerization (DP), and the number-average molecular weight (M_n) were by end-group analysis of the ^{1}H NMR spectra and confirmed by MALDI-TOF-MS (Supporting Information). [d]Polymer concentration that induced 50% leakage of hemoglobin from human red blood cells (HC_{50}) relative to the positive control surfactant Triton-X-100. The data are rounded to two significant digits.

Polymer Characterization. ^{1}H NMR confirmed that the copolymers were obtained and that there was no detectable amount of unreacted monomer or chain transfer agent remaining in the samples. Comparison of the integrated peak areas enabled calculation of the number-average degrees of polymerization (DPs), based on end group analysis, and the average mole fraction of hydrophobic repeating units (f_{HB}) was determined. MALDI-TOF-MS wasperformed with a Micromass TofSpec-2E spectrometer in linear positive ion mode with a 20 kV potential. The matrix was α-cyano-4-hydroxycinnamic acid in ethanol/acetonitrile (10 mg/mL). Polymer solutions (1 mM, 1 uL) and matrix solution (10 uL) were spotted onto the target plate. MW distributions matched the NMR calculation (Supporting Information).

Antimicrobial Activity. The lowest polymer concentration required to inhibit growth of bacteria completely, defined as the MIC, was determined by a turbidity-based microdilution assay in Muller Hinton (MH) broth according to the procedure approved by The National Committee for Clinical Laboratory Standards (NCCLS) with the modifications proposed by Weigand et al.[34] An overnight culture of bacterial strains was regrown to exponential phase (OD_{600} of 0.5 to 0.6) and diluted to OD_{600} = 0.001 in MH broth. This stock (90 μL) was mixed with a polymer solution (10 μL) in a 96-well polypropylene microplate (Corning no. 3359) to give the final concentration of bacteria on the microplate of approximately 5×10^5 CFU/mL. After incubating for 18 h at 37 °C, the OD_{600} in each well was recorded using a microplate reader (Perkin-Elmer Lambda Reader). The MIC was defined as the lowest polymer concentration at which no turbidity increase was observed relative to the negative control, MH broth. All experiments were performed three times in triplicate, and the MIC values reported are the average of the three trials. The MIC values were determined below the solubility limit of the polymers in MH broth in every case.

Bactericidal kinetics was determined by inoculation of the polymers with bacteria in MH broth and colony counting on agar plates. An overnight culture of *E. coli* ATCC 25922 was regrown to exponential phase (OD_{600} of 0.5 to 0.6) and diluted to an OD_{600} of 0.001 in 8 mL of MH broth, and polymer was added from stock solution to a final concentration of two times the MIC value (Table 1). The tubes were incubated at 37 °C with orbital shaking and 10 μL aliquots were drawn every 15 or 30 min. After dilution by 10^3, 10^2, or 10-fold in buffer, the cells were streaked onto agar plates and incubated overnight. The colonies were then counted to determine the cfu/mL as a function of time. Each data point was done in duplicate, and the averages are reported plus or minus the range.

Hemolytic Activity. Toxicity to human RBCs was assessed by a hemoglobin release assay. RBCs (1 mL) were diluted into HEPES buffered saline (9 mL; HBS = 10 mM HEPES, 150 mM NaCl, pH 7) and washed with HBS three times. The stock (10% v/v) was diluted three-fold in HBS (3.3% v/v) and was then mixed (90 μL) with polymer solution (10 μL) on a 96-well microplate (final 3% v/v, 10^8 RBC/mL). After 60 min of incubation at 37 °C and 100 rpm, the plate was centrifuged at 1000 rpm for 10 min, and the supernatant (10 μL) was diluted into PBS (90 μL). Absorbance at 405 nm was recorded using a microplate reader (Perkin-Elmer Lambda Reader). The fraction of hemolysis was defined as $H = (A - A_0)/(A_{TX} - A_0)$, where A is the absorbance reading of the sample well, A_0 is the negative hemolysis control (buffer), and A_{TX} is the positive hemolysis control (Triton X-100). HC_{50} was defined as the polymer concentration that causes 50% hemolysis by curve-fitting with the empirical Hill equation, $H = 1/((HC_{50}/[P])^n + 1)$, where $[P]$ is the total concentration of polymer and the fitting parameters were n and HC_{50}. All experiments were performed three times in triplicate.

Molecular Dynamics Simulations. Model copolymers with DP = 10 and f_{HB} = 0.3 (Figure 7) were inserted in aqueous phase above pre-equilibrated POPE-POPG (7:3) bilayers, and each system (three in total) was simulated for 100 ns. Counterions were added to each system for overall charge neutrality. All three systems were simulated under isothermal−isobaric ensemble conditions (305 K temperature and 1 atm pressure). The long-range Coulomb interactions were dealt with particle mesh Ewald method. An integration time step of 1.0 fs was used for the first 10 ns, and a time step of 2 fs was used for all subsequent runs. All simulations were performed by NAMD2.7.[35] The forcefield parameters for polymers were adopted from our previous simulations,[36] the latest forcefield of CHARMM36[37] was used for lipids, and water was modeled by TIP3P model.[38]

RESULTS AND DISCUSSION

Polymer Synthesis and Characterization. Random copolymers of Boc-protected aminoalkylmethacrylates and EMA were prepared by thermally initiated free radical polymerization in the presence of the chain transfer agent methyl mercaptopropionate to afford low-MW (<10 kDa) copolymers. The procedure was modified from the previously described protocol.[23] As a preliminary experiment, the copolymerization was monitored by drawing aliquots at regular intervals and determining the conversion of each comonomer by gas chromatography, relative to the internal standard mesitylene. For each pair of comonomers (1:1 ratio), both methacrylates were consumed at nearly identical rates, suggesting the random incorporation of monomers to the polymer chain regardless of the side-chain spacer length of aminoalkylmethacrylates (Figure 1). GPC revealed that the MWs (5 to 6 kDa) and polydispersity index (PDI) values (1.5 to 1.6) of the obtained copolymers with different spacer arms are comparable. Hence, we synthesized an extensive library of random copolymers containing various ratios of hydrophobic to amino-functionalized methacrylate repeating units for bioactivity assessment (Figure 2).

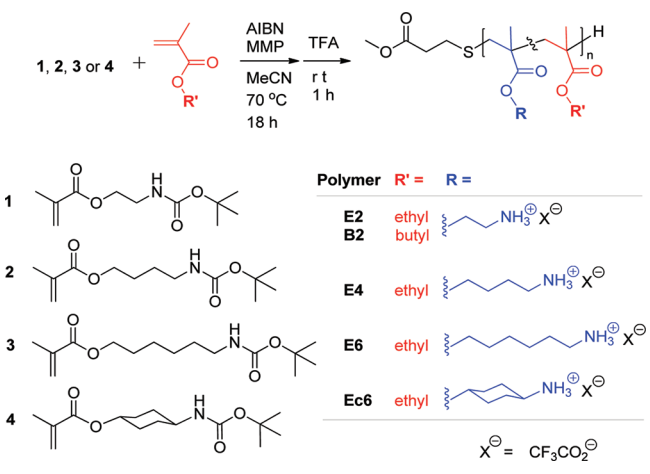

Figure 2. Synthesis of cationic, amphiphilic methacrylate random copolymers with various cationic side chain spacer arms. AIBN: 2,2′-Azobis(2-methylpropionitrile). MMP: Methyl mercaptopropipnate. MeCN: Acetonitrile.

Deprotection of the copolymers was achieved using TFA (Figure 2), and the obtained cationic, amphiphilic copolymers were characterized by ^{1}H NMR. The average DPs were calculated based on comparison of the integrated peak areas arising from the methyl ester end groups and the side chains (Supporting Information Figure S1). Although GPC could not be performed on the cationic copolymers because of their insolubility in THF, the MALDI-TOF-MS of representative deprotected copolymers corroborates the NMR end-group analysis (Supporting Information Figure S2). We intentionally tailored the average DPs to the range of 12−15 (Table 1) because such low-MW polymers in this range have been previously shown to give potent antimicrobial activity with

minimal hemolysis, whereas increasing MW generally increases hemolysis.[15]

The f_{HB} values were obtained by comparison of signals arising from the two different side chains in the ^{1}H NMR spectra. For each copolymer series, the fraction of hydrophobic repeat units (EMA or BMA) in the copolymer, f_{HB}, was varied in the range of 0.0 to 0.6. Copolymers with higher f_{HB} values were not studied because of insolubility in the aqueous assay media. The ammonium side-chain spacer arms were varied from ethylene (E2), butylene (E4), hexylene (E6), to cyclohexylene (Ec6). The f_{HB} values of each of the polymers are indicated by the subscript for each sample (Table 1). For example, the copolymer in the E4 series containing 29 mol % EMA units is referred to as $E4_{29}$.

Potentiometric Titration. The ionization behavior of the polymers in this study was assessed by potentiometric titration (Figure 3).[39−41] The adjustment of the spacer groups

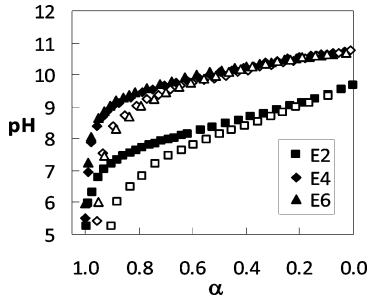

Figure 3. Ionization behavior of the cationic homopolymers containing various "spacer arms" by potentiometric titration. Forward titration with NaOH (filled symbols) and back-titration with HCl (open symbols).

significantly impacted the titration curves: about 30% of the primary amine groups in the homopolymer $E2_0$ were deprotonated at pH 8, whereas <5% of the amine groups in $E4_0$ and $E6_0$ were deprotonated at pH 9. The effect of increasing apparent pK_a (pH at α = 0.5) with elongated spacer length is in agreement with a previous report on related amino-functionalized methacrylates.[42] Columbic repulsion of neighboring charges localized in the polymer chains increases the repulsive energy between side chains, reducing the degree of protonation compared with the monomers in solution.[43] Elongation of the spacer arms allows for greater spatial separation of the ammonium groups on neighboring monomer units, relieving the Columbic repulsion and thereby increasing the apparent pK_a values. The elongation of cationic side chain groups has also been utilized to control side-chain interactions, resulting in enhancement of the formation of secondary structures of synthetic peptides.[44] The biological activity assays are performed at pH 7, in which >93% of the amino groups in all of the homopolymers are protonated (cationic).

The forward- and back-titration data deviate as α is increased beyond about 0.5. On the basis of our previous work[39] and others,[43] this deviation is likely a result of isomerization of the aminoalkylmethacrylate units to hydroxyalkylmethacrylamide units or hydrolysis of the side-chain ester groups, which reduces the number of amine groups in the polymer and curtails activity. Despite the instability of the amino-methacrylates at pH >9, the polymers are chemically stable up to pH 8 at 37 °C overnight. Moreover, the elongation of spacer groups appears to suppress the isomerization reactions to some extent, as evidenced by more closely matched forward and back-titration data curves. This may be due to the fact that longer linkages separate the amine groups from the esters in the backbone, reducing the likelihood of intramolecular nucleophilic addition.

Antimicrobial Activity. The antimicrobial activities of the polymers were quantified in terms of MIC, the lowest polymer concentration that completely inhibits bacterial growth. The MIC values were determined in a turbidity-based microdilution assay. See the Supporting Information (Table S1) for MIC values of the entire library of copolymers in this work. In general, the copolymers in this study exhibited inhibitory effects against Gram negative *E. coli* and Gram positive *S. aureus* to varying extents depending on their cationic side-chain spacer arm groups and their f_{HB} values (Table 1 and Figure 4).

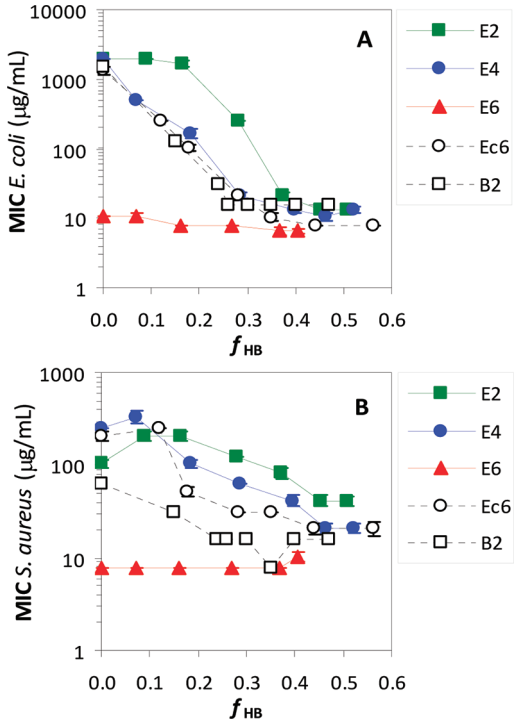

Figure 4. Antimicrobial activity of the copolymers with various spacer arms and comonomer compositions, against *E. coli* and *S. aureus*. Minimum inhibitory concentration (MIC) is defined the lowest polymer concentration, which completely inhibits the growth of bacteria based on turbidity. The initial challenge was ~5 × 10^5 cfu/mL. Error bars represent the standard deviation from three independent trials, each done in triplicate.

The spacer groups strongly impacted the antimicrobial activity of the polymers against *E. coli* (Table 1 and Figure 4). The cationic homopolymers $E2_0$ and $E4_0$ showed only weak antimicrobial activity against *E. coli* (MIC = 2000 μg/mL), whereas $E6_0$ exhibited an MIC value of 10 μg/mL. This suggests that elongation of spacer length enhances the activity of the cationic homopolymers without incorporation of hydrophobic comonomers. For comparison, the bee venom toxin peptide melittin and natural AMP magainin-2 displayed an MIC value of 12 and 125 μg/mL against *E. coli*, respectively. It should be noted that homopolymers $E2_0$ and $B2_0$ have the same chemical structures, but the $B2_0$ displayed lower MIC values. This is likely to reflect the higher MW of $B2_0$.[39]

The weak activity of E2 and E4 homopolymers may suggest that the hydrophobic properties of polymers are not sufficient

to exert their antibacterial effect.[23] Hence, we further examined the effect of increasing the fraction of hydrophobic comonomer (f_{HB}) content on the activity. The MIC values generally decreased with increasing f_{HB}, except for the E6 polymers, which displayed no dependence of MIC on f_{HB}. When the hydrophobic content is increased beyond f_{HB} = 0.4, the MIC values reached a plateau of ~10 μg/mL for all polymers. This indicates that the hydrophobic properties of the comonomer EMA dominate the activity over the effect of spacer arm length when the fraction of hydrophobic comonomer exceeds ~0.4. The effect of spacer arm length is quite evident when 0.1 < f_{HB} < 0.4, where the MIC values of copolymers decreased by orders of magnitude as the spacer arms were elongated from two (E2) to six (E6) carbon linkages. For example, elongating the spacer arms from two ($E2_{28}$) to four ($E4_{29}$) carbon atoms led to a decrease in MIC from 250 to 20 μg/mL, an activity enhancement of about 12-fold (Table 1). Further extension of the spacer arms to six carbons ($E6_{27}$) yielded an MIC value of ~8 μg/mL. We speculate that the hydrophobic property of the 6-aminohexyl side chains dominates the activity, whereas the comomoner EMA has no impact on the activity in this particular case. In the moderate range of hydrophobic comonomer EMA content (f_{HB} = 0.27 to 0.29) the relative activity ranking is $E6_{27}$ > $E4_{29}$ > $E2_{28}$, supporting the notion that the antibacterial activity can be controlled by the combination of spacer arm elongation and the hydrophobic comomomers.

Interestingly, the MICs of Ec6, which possesses constrained cyclohexyl spacer arms, are orders of magnitudes weaker than those of E6, whereas these polymers contain the same number of carbon atoms (C6) in their spacer groups, This indicates that the antibacterial mechanism is sensitive to structural difference and properties of spacer arms (cyclic vs linear alkyl).

Against *S. aureus*, similar to the case of *E. coli*, the MIC values decreased with increasing f_{HB} and reached a plateau of ~10−20 μg/mL for all the copolymers (Figure 4B). The MIC values of hompolymers and copolymers with low f_{HB} for *S. aureus* are lower than *E. coli*, indicating that *S. aureus* is more susceptible to the cationic polymers. For the copolymers with hydrophobic content in the range of f_{HB} = 0.27 to 0.29, the antimicrobial activity increased with increasing spacer group length, giving the relative activity ranking: $E6_{27}$ > $E4_{29}$ > $E2_{28}$. These results also demonstrate that the activity against Gram positive *E. coli* as well as Gram negative *S. aureus* can be controlled by tuning the spacer arm groups in the cationic side chains.

Hemolytic Activity. Damage to human RBCs was quantified as the polymer concentration that induces 50% hemoglobin release (HC_{50}), which was determined from dose−response curves, that is, the percentage of hemolysis measured as a function of polymer concentration. (See Figure S4 in the Supporting Information for hemolysis dose−response curves of all of the copolymers in this study.)

The homopolymers in all but the E6 series were relatively nonhemolytic (HC_{50} > 2000 ug/mL) (Figure 5). For comparison, the bee venom toxin peptide melittin showed an HC_{50} value of 1.7 μg/mL under this assay condition. The hemolysis increased by orders of magnitude with increasing f_{HB}, from 0 to ~0.5, for all copolymers except E6 polymers, which showed constant HC_{50} value of ~5 μg/mL regardless of the f_{HB} values. When the hydrophobic comonomer EMA composition was increased excessively (f_{HB} > 0.5), the hemolytic activity of all copolymers was pronounced, with HC_{50} < 20 μg/mL without a large dependence on the identity of the spacer arm

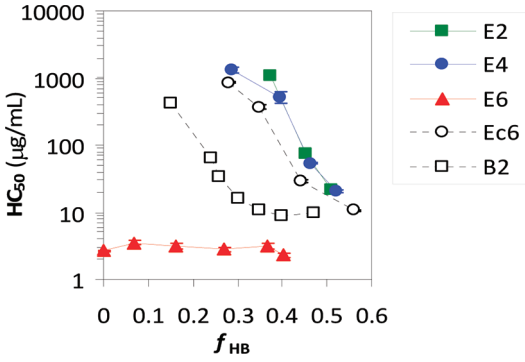

Figure 5. Hemolytic activity of the copolymers with various spacer arms and comonomer compositions against human red blood cells. Error bars represent the standard deviation from three independent trials, each done in triplicate.

groups. It appears that the hemolytic activity of copolymers may be approaching a plateau region at high hydrophobicity, although it was not possible to confirm this with polymers of higher f_{HB} because of their insolubility in the assay media.

The copolymer $E4_{29}$ showed potent antimicrobial activity (MIC = 21 μg/mL for *E. coli*) but was relatively nonhemolytic (HC_{50} = 1300 μg/mL), giving a selectivity index (HC_{50}/MIC) of 63 (Table 1 and Figure 6). In the E2 polymer series, the best

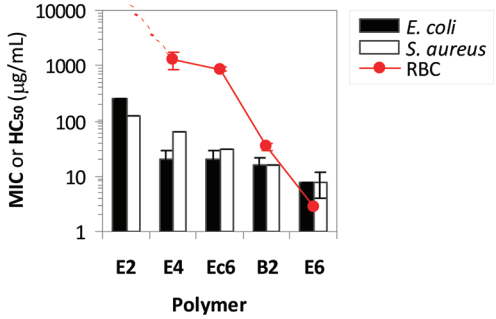

Figure 6. Selectivity of the copolymers containing various cationic side chain spacer arms, for *E. coli* and *S. aureus* relative to human red blood cells.

example was $E2_{37}$, which showed potent antimicrobial activity (MIC = 21 μg/mL) and relatively weak hemolytic activity (HC_{50} = 1100 μg/mL), giving a selectivity index of 52. The E6 copolymers showed high hemolytic activity (HC_{50} < 5 μg/mL) and very low selectivity (HC_{50}/MIC < 1) regardless of the f_{HB} values. The B2 polymers, which contain BMA comonomers as the hydrophobic groups, have been previously reported[23] to show the potent activity with relatively low selectivity toward bacteria over human RBCs. The MIC values of $B2_{26}$ are similar to those of $E4_{29}$ (MIC = 15−20 μg/mL), but $B2_{26}$ is highly hemolytic (HC_{50} = 34 μg/mL). These results demonstrate that the copolymers can be tuned by selecting ethylene or butylene spacer arms and relatively low f_{HB} to inhibit bacterial growth selectively without causing adverse toxicity to human RBCs.

We speculate that the spacer arms would enable fine-tuning of the hydrophobic property of polymers, which provides an additional design strategy to obtain balanced amphiphilic properties such that these polymers exert selective activity against bacteria over RBCs. We also speculate that the spacer arms play an important role in the binding of polymers to cell

membranes and polymer conformations in membranes, which will be discussed in the following section.

Bactericidal Kinetics. We further examined the bactericidal kinetic exerted by representative copolymers, which displayed potent antibacterial activity but varying degrees of selectivity to bacteria over RBCs (Figure 6) to assess the potential of thee copolymers as antibacterial agents. Accordingly, we monitored the number of viable *E. coli* cells as a function of exposure time to the copolymers at twice their respective MIC concentrations. $E4_{29}$ and $E6_{27}$ caused three-log reductions in the viable cell population (99.9% killing) within 60 and 15 min, respectively, whereas $E2_{28}$ required 120 min for the same level of reduction (Figure 7). This demonstrates that the rate of killing was

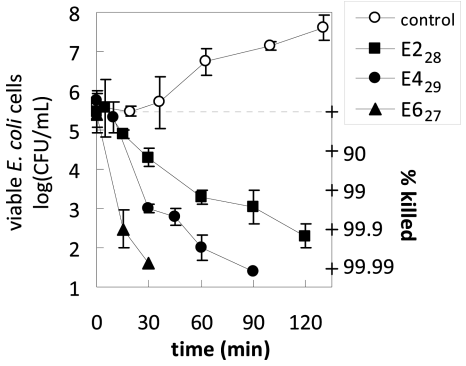

Figure 7. Bactericidal kinetics by copolymers. The concentration of viable *E. coli* cells given in colony-forming units per milliliter (CFU/mL) (left *y*-axis) or the percentages of killed *E. coli* (right *y*-axis) after incubation with the copolymers was plotted as a function of time. Three representative copolymers ($E2_{28}$, $E4_{29}$, and $E6_{27}$) containing different spacer arms with f_{HB} in the range of 0.27 to 0.29 were used in this assay. The initial *E. coli* concentration was ~4.5×10^5 CFU/mL, and the polymer concentrations were twice their respective MIC values (MIC = 250, 21, and 7.8 μg/mL for $E2_{28}$, $E4_{29}$, and $E6_{27}$, respectively). Error bars represent the range from duplicate measurements.

accelerated by the elongation of the spacer groups, in corroboration with the observed decrease in MIC values. By comparison, Pexiganin, a potent synthetic derivative of magainin, was reported to cause a 3-log reduction in the viable *E. coli* cell population within 1 h at a concentration of twice the MIC.[10] The copolymers in this study appear to exert similar bactericidal effect.

Activity Spectrum. To assess the spectrum of activity, we also tested the representative copolymers against a panel of Gram positive and Gram negative bacteria (Table 2). The MIC values of $E4_{29}$ are equal to or less than 100 μg/mL for all of the tested strains, which is substantially lower than the HC_{50} value (1300 μg/mL). These results suggest that the copolymer has the broad spectrum activity with selective activity to bacteria over human RBCs. For all of the strains tested, elongation of the spacer arm side-chain length caused an improvement in the antimicrobial activity. Importantly, the E4 copolymers showed inhibitory effects against *A. baumannii*, which is inherently resistant to many antibiotic drugs,[45] and a community-acquired strain of methicillin-resistant *S. aureus* (MRSA)[46] at low microgram per milliliter concentrations.

Molecular Dynamics Simulation. Although molecular-level details of the bactericidal action exerted by polymers and peptides have been elusive experimentally, simulations have provided a wealth of information on this fine scale. Accordingly,

Table 2. Spectrum of Antimicrobial Activity by Representative Copolymers

		MIC or HC_{50} (μg/mL)				
bacterium	gram	$E2_{28}$	$E4_{29}$	$E6_{27}$	melittin[b]	magainin-2[b]
Staphylococcus aureus	(+)	125	63	7.8	5.6	>250
Staphylococcus aureus (CA-MRSA)[a]	(+)	125	31	7.8	n.d.	n.d.
Enterococcus faecalis	(+)	250	31	7.8	16	>500
Bacillus subtilis	(+)	31	7.8	3.9	5.6	63
Escherichia coli	(−)	250	21	7.8	12	125
Acinetobacter baumannii	(−)	63	10	3.9	n.d.	n.d.
Pseudomonas aeruginosa	(−)	210	16	16	280	500
Salmonella enterica	(−)	125	16	7.8	140	500
human RBC (HC_{50})		>2000	1300	2.8	1.7	>250

[a]Community acquired methicillin-resistant *S. aureus* (MRSA) strain LAC 1263. [b]MIC values were previously reported.[47]

we modeled the interaction of three representative copolymers (E2, E4, and E6) with lipid membranes by molecular dynamics simulations. The structures used for these simulations are copolymers with DP = 10 and f_{HB} = 0.3 (Figure 8). The mole

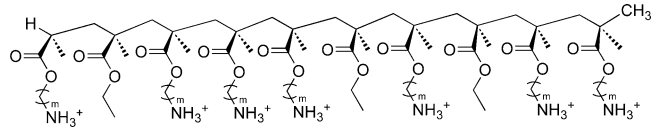

Figure 8. Monomer sequence and structures of model copolymers. The copolymers have different length of cationic spacer arms: ethylene (m = 2) for $E2_{model}$, butylene (m = 4) for $E4_{model}$, and hexane (m = 6) for $E6_{model}$.

fraction f_{HB} = 0.3 was selected because the polymers that showed antimicrobial and hemolytic activities in this range were sensitive to the spacer arms in the side chains. We modeled the copolymer structures with an isotactic sequence in which cationic monomers and EMA comonomers were unevenly distributed, or scrambled, in a ratio of 7:3.

The model membranes selected to understand the interactions of the three model polymers with lipid bilayers are composed of POPE and POPG lipids in a 7:3 ratio, which is a common formulation used to mimic bacterial cell membranes.[48] In all three simulations, the polymer backbones are seen to be parallel to the membrane surface, with the hydrophobic groups projected into the membrane core and the ammonium groups projected to the water−membrane interface (Figure 9). It appears that the depth of insertion depends on the spacer arm length. The copolymer $E2_{model}$ (the model polymer with m = 2 in Figure 8) was found to be largely near the lipid membrane surface, and most of the ammonium groups (colored orange) appear to remain in water phase even at the end of 100 ns of simulation. $E2_{model}$ also adopted a stable compact conformation such that the polymer chain is folded in the *XY* plane (perpendicular to membrane normal) (Figure 9B). The cationic ammonium groups in the polymer side chains (colored red) of $E4_{model}$ and $E6_{model}$ are localized at the lipid−

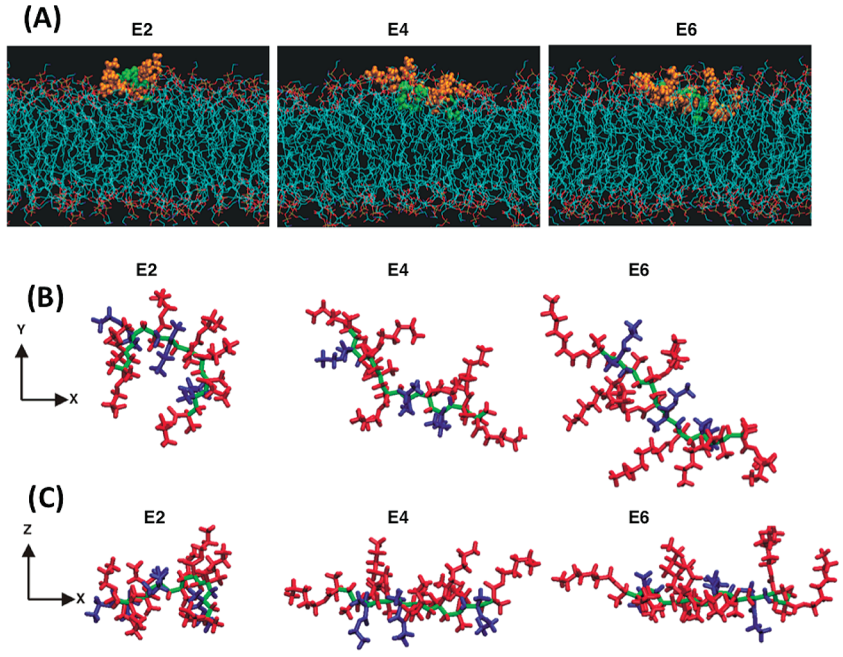

Figure 9. (A) Snapshots of the three systems at the end of 100 ns simulations. Water is not shown for clarity. The ammonium spacer arm groups and hydrophobic ethyl groups of EMA comonomers are colored orange and green, respectively. (B) Average conformation of the copolymers in the *XY* plane (perpendicular to membrane normal) at the end of 100 ns of MD simulations. The cationic and EMA ethyl side chains are colored red and blue, respectively. The polymer backbones are colored green. (C) Average conformation of the copolymers oriented parallel to the membrane normal.

water interface, and the nonpolar ethyl side chains of comonomer EMA (colored green) are inserted into the hydrophobic membrane core (Figure 8). The end-to-end distances of the polymers in the last 20 ns of simulation are ~20 Å for $E4_{model}$ and $E6_{model}$ (Figure S5 of the Supporting Information), indicating that $E4_{model}$ and $E6_{model}$ are in highly stretched conformations, considering that the theoretical length for a fully extended conformation is 23 to 24 Å. The cationic spacer arms and hydrophobic ethyl groups of EMA comonomer in the polymer side chains are segregated to opposite faces of the polymer backbone (Figure 9C). The average distances between the center of mass of the ethyl and amine groups in the polymers are ~7 and ~9 Å for $E4_{model}$ and $E6_{model}$ (Figure S6 of the Supporting Information), which are substantial given that the theoretical maximum distances for full extension are ~16 and ~18 Å, respectively.

The Z-density profiles of the copolymers also illustrate amphiphilic conformations in the lipid bilayer upon polymer insertion. The ammonium groups of the polymer side chains (Figure 10, black line) are well-aligned with the phosphate heads groups of both lipids (blue line) and the hydroxyl groups of POPG glycerol (purple line), suggesting that the ammonium groups are localized near the water–membrane interface. The peaks of the ethyl side chains (green line) and the lipid acyl chains (orange) also overlap, indicating that the hydrophobic side chains of the polymer are inserted into the hydrophobic membrane core. The ammonium groups in the side chains and the ethyl side chains are spatially segregated with respect to the ester groups of side chains (red line) for $E4_{model}$ and $E6_{model}$, indicating that the cationic arms and ethyl side chains are presented on opposite faces of the polymer backbone.

These results suggest that these polymers adopt facially amphiphilic conformations upon binding to the membranes despite their lack of defined intrinsic secondary structures such

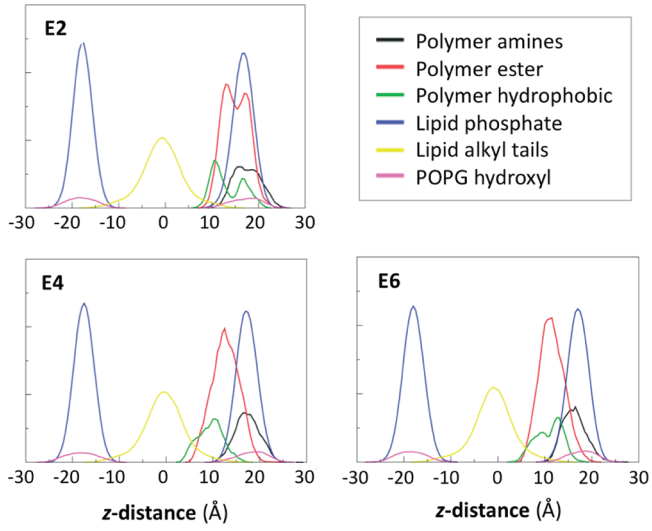

Figure 10. Z-density profiles of various components of lipid–polymer systems averaged over last 20 ns of MD simulations. The green lines represent the polymer hydrophobic side chains, whereas the black lines denote the polymer amino groups. Clearly, the segregation into facially amphiphilic conformations is evident in the case of the E2 and E4 model copolymers.

as α-helix and β-sheet found in naturally occurring AMPs. Mondal et al. previously investigated the interaction of helical β-peptides and random copolymer models of β-peptides with a model membrane[49] and suggested that these peptides bind to the membrane by forming facially amphiphilic structures. The analysis of peptide sequence and conformation in that study implied that well-defined secondary structure is not necessary for peptide binding, and the ability of peptide sequence to segregate the cationic and hydrophobic groups is rather

dx.doi.org/10.1021/bm300342u | *Biomacromolecules* 2012, 13, 1632–1641

important for efficient binding. Despite the distinctive differences in the chemical structures and conformational restriction (backbone flexibility) between the peptides and the methacrylate copolymers studied here the same principle appears to govern the polymer-membrane binding.

The copolymer chains are positioned more toward the hydrophobic membrane core as the spacer arms are elongated (Figure 9). By analogy to the snorkel effect observed with transmembrane peptide helices,[30−32] we expected that increased spatial separation between the cationic ammonium and hydrophobic ester groups would facilitate deeper membrane insertion. Indeed, the distribution of ester groups (red line) also shifted toward the center of the lipid bilayer as the spacer side chains were elongated (Figure 10). The longer alkyl chain in the spacer arms could provide more hydrophobicity for membrane insertion as well as additional distance between the cationic side chains and the hydrophobic polymer backbone, by analogy to the snorkeling effect observed in peptides.[29] The snorkeling effect reduces the energetic barrier to peptide insertion for transmembrane helices. Studies on such peptides indicated that the butylene side-chain spacer arms of lysine residues facilitate such insertion. In this study, variation of spacer arm alkyl length enables control of polymer insertion as well. It has been suggested that the smaller conformational restriction on the cationic segments of β-peptides results in the lower free energy for attachment to membranes.[49] The longer spacer arms of methacrylate copolymers may facilitate the arrangement into facially amphiphilic coils due to an increase in conformational freedom in the cationic side chains. This may in turn enable the deeper insertion of polymer chains into the membranes as well as lowering the free energy barrier to membrane binding. However, the $E4_{model}$ and $E6_{model}$ copolymers do not appear to penetrate entirely to the membrane core. One possibility is that the hydrophobic ethyl groups of comonomers are not inserted into the membrane to significant extent because the ethyl ester groups of EMA are not hydrophobic enough for deeper insertion. We also speculate that the ester groups of methacrylate are not optimal for membrane insertion because the polarity of ester groups costs energy, not favorable to be buried into the hydrophobic membrane core.

It is interesting to note that $E2_{model}$ adopted a folded conformation in the *XY* plane, whereas $E4_{model}$ and $E6_{model}$ showed more extended backbones (Figure 9B). This is likely due to the polarity of the lipid−water interface, which determines the polymer conformations. Because $E2_{model}$ is located at the lipid−water interface, the polymer chain folds into the compact conformation to minimize the exposure of hydrophobic polymer backbone and side chains to the aqueous phase, similar to micelle formation in aqueous solution. $E4_{model}$ and $E6_{model}$ are inserted into the hydrophobic membrane core, which in turn makes the polymer chains extend to maximize the interaction between the polymer backbone and acyl chains of lipids. The detailed analysis of polymer conformation and membrane insertion will be discussed in a forthcoming report. These results suggest that the spacer arms could modulate the polymer binding to membranes and amphiphilic conformation. The applicability of this polymer-membrane binding model to the biological activity remains tentative at this time. Several mechanisms have been proposed to explain the membrane-disrupting action of AMPs. The proposed models suggest that multiple α-helical peptides either insert into cell membranes to form transmembrane pores cooperatively or accumulate on the cell surface to disintegrate the membrane integrity.[4] Interestingly, a computational study on the action of magainin derivatives in lipid bilayer showed that they were able to form distorted toroidal pores even when the peptides were not in a stable α-helix form.[50] This indicates that an α-helical conformation is not a prerequisite for pore formation. Further investigation on the polymer binding and cooperativity between multiple synthetic polymer chains would therefore enhance our understanding of the membrane disruption mechanism and biological relevance. Elucidating the relationship between chemical structures of the copolymers and their interactions with membranes is requisite for the rational design of optimal copolymer structures for potent activity.

■ CONCLUSIONS

We developed a new strategy to modulate the antimicrobial and hemolytic activities of amphiphilic random copolymers by adjustment of the cationic side-chain spacer arms. In terms of potent antimicrobial activity (MIC in low μg/mL) and minimal hemolytic activity, the four carbon spacer arms in 4-aminobutylmethacrylate afford the best profile in this study. This polymer exerts relatively rapid bactericidal kinetics and shows broad-spectrum activity against a panel of bacteria, including MRSA and *A. baumannii*.

Preliminary studies by molecular dynamics simulations showed that the copolymers adopt segregation of cationic side chains and ethyl groups of comonomer EMA or facially amphiphilic conformation when bound to a bacteria-type lipid membrane. The formation of such amphiphilic polymer conformations might be a key determinant for optimal antimicrobial efficacy, although exact details of the antibacterial mechanism of polymers remain unclear at this point. In the case of designing AMPs, MD simulations have been called upon to explain and predict biological activity profiles.[49] In the future, MD simulations may also aid in the understanding of the biological activities observed in synthetic polymers as well as rational design of membrane-active antimicrobial polymers. This spacer arm approach will provide new molecular design strategy to improve the antibacterial activity of amphiphilic random copolymers as well as to shed light to the mechanism of antibacterial action of polymers.

■ ASSOCIATED CONTENT

Supporting Information

Polymer synthesis and characterization data and supplementary biological activity data. This material is available free of charge via the Internet at http://pubs.acs.org

■ AUTHOR INFORMATION

Corresponding Author

*E-mail: vani@imsc.res.in (S.V.) and kkuroda@umich.edu (K.K.).

Notes

The authors declare the following competing financial interest(s): K. Kuroda is a coinventor on a patent application filed by the University of Pennsylvania covering "Antimicrobial Copolymers and Uses Thereof". The patent application has been licensed to PolyMedix, Inc. (Radnor, PA). PolyMedix did not play a role in the design and conduct of this study, in the collection, analysis, or interpretation of the data, or in the preparation, review, or approval of the article.

■ ACKNOWLEDGMENTS

This research was supported by the Department of Biologic and Materials Sciences, University of Michigan School of Dentistry and NSF CAREER Award (DMR-0845592 to K.K.). For the MD simulations, computing time on the "Annapurna" cluster at IMSc is greatly appreciated. We thank Dr. Robertson Davenport, University of Michigan Hospital, for providing the RBCs, Prof. Eric Krukonis, University of Michigan School of Dentistry for use of the microplate reader, Prof. Blaise Boles at University of Michigan for providing MRSA LAC 1263, and Prof. Anne J. McNeil, University of Michigan Chemistry Department, for use of the GPC and GC.

■ REFERENCES

(1) Boucher, H. W.; Talbot, G. H.; Bradley, J. S.; Edwards, J. E.; Gilbert, D.; Rice, L. B.; Scheld, M.; Spellberg, B.; Bartlett, J. *Clin. Infect. Dis.* **2009**, *48* (1), 1−12.
(2) Zasloff, M. *Nature* **2002**, *415* (6870), 389−395.
(3) Marr, A. K.; Gooderham, W. J.; Hancock, R. E. W. *Curr. Opin. Pharmacol.* **2006**, *6* (5), 468−472.
(4) Brogden, K. A. *Nat. Rev. Microbiol.* **2005**, *3* (3), 238−250.
(5) Marcos, J. F.; Gandia, M. *Expert Opin. Drug Discovery* **2009**, *4* (6), 659−671.
(6) Yeaman, M. R.; Yount, N. Y. *Pharmacol. Rev.* **2003**, *55* (1), 27−55.
(7) Bader, M. W.; Navarre, W. W.; Shiau, W.; Nikaido, H.; Frye, J. G.; McClelland, M.; Fang, F. C.; Miller, S. I. *Mol. Microbiol.* **2003**, *50* (1), 219−230.
(8) Gooderham, W. J.; Bains, M.; McPhee, J. B.; Wiegand, I.; Hancock, R. E. W. *J. Bacteriol.* **2008**, *190* (16), 5624−5634.
(9) Matsuzaki, K. *Biochim. Biophys. Acta, Biomembr.* **2009**, *1788* (8), 1687−1692.
(10) Ge, Y. G.; MacDonald, D. L.; Holroyd, K. J.; Thornsberry, C.; Wexler, H.; Zasloff, M. *Antimicrob. Agents Chemother.* **1999**, *43* (4), 782−788.
(11) Patch, J. A.; Barron, A. E. *J. Am. Chem. Soc.* **2003**, *125* (40), 12092−12093.
(12) Tew, G. N.; Scott, R. W.; Klein, M. L.; Degrado, W. F. *Acc. Chem. Res.* **2010**, *43* (1), 30−39.
(13) Liu, D. H.; Choi, S.; Chen, B.; Doerksen, R. J.; Clements, D. J.; Winkler, J. D.; Klein, M. L.; DeGrado, W. F. *Angew. Chem., Int. Ed.* **2004**, *43* (9), 1158−1162.
(14) Ilker, M. F.; Nusslein, K.; Tew, G. N.; Coughlin, E. B. *J. Am. Chem. Soc.* **2004**, *126* (48), 15870−15875.
(15) Kuroda, K.; Caputo, G. A.; DeGrado, W. F. *Chem.—Eur. J.* **2009**, *15* (5), 1123−1133.
(16) Mowery, B. P.; Lee, S. E.; Kissounko, D. A.; Epand, R. F.; Epand, R. M.; Weisblum, B.; Stahl, S. S.; Gellman, S. H. *J. Am. Chem. Soc.* **2007**, *129* (50), 15474−15476.
(17) Rathinakumar, R.; Walkenhorst, W. F.; Wimley, W. C. *J. Am. Chem. Soc.* **2009**, *131* (22), 7609−7617.
(18) Wimley, W. C. *ACS Chem. Biol.* **2010**, *5* (10), 905−917.
(19) Matsuzaki, K.; Harada, M.; Funakoshi, S.; Fujii, N.; Miyajima, K. *Biochim. Biophys. Acta* **1991**, *1063* (1), 162−170.
(20) Wakamatsu, K.; Takeda, A.; Tachi, T.; Matsuzaki, K. *Biopolymers* **2002**, *64* (6), 314−327.
(21) Cheng, R. P.; Gellman, S. H.; DeGrado, W. F. *Chem. Rev.* **2001**, *101* (10), 3219−3232.
(22) Porter, E. A.; Wang, X.; Lee, H. S.; Weisblum, B.; Gellman, S. H. *Nature* **2000**, *405* (6784), 298−298.
(23) Kuroda, K.; DeGrado, W. F. *J. Am. Chem. Soc.* **2005**, *127* (12), 4128−4129.
(24) Palermo, E. F.; Sovadinova, I.; Kuroda, K. *Biomacromolecules* **2009**, *10* (11), 3098−3107.
(25) Mowery, B. P.; Lindner, A. H.; Weisblum, B.; Stahl, S. S.; Gellman, S. H. *J. Am. Chem. Soc.* **2009**, *131* (28), 9735−9745.
(26) Palermo, E. F.; Lee, D.-K.; Ramamoorthy, A.; Kuroda, K. *J. Phys. Chem. B* **2011**, *115*, 366−375.
(27) Avery, C. W.; Palermo, E. F.; McLaughin, A.; Kuroda, K.; Chen, Z. *Anal. Chem.* **2011**, *83* (4), 1342−1349.
(28) Monne, M.; Nilsson, I.; Johansson, M.; Elmhed, N.; von Heijne, G. *J. Mol. Biol.* **1998**, *284* (4), 1177−1183.
(29) Mishra, V. K.; Palgunachari, M. N.; Segrest, J. P.; Anantharamaiah, G. M. *J. Biol. Chem.* **1994**, *269* (10), 7185−7191.
(30) Jaud, S.; Fernandez-Vidal, M.; Nilsson, I.; Meindi-Beinker, N. M.; Hubner, N. C.; Tobias, D. J.; von Heijne, G.; White, S. H. *Proc. Natl. Acad. Sci. U.S.A.* **2009**, *106* (28), 11588−11593.
(31) Schow, E. V.; Freites, J. A.; Cheng, P.; Bernsel, A.; von Heijne, G.; White, S. H.; Tobias, D. J. *J. Membr. Biol.* **2011**, *239* (1−2), 35−48.
(32) Krishnakumar, S. S.; London, E. *J. Mol. Biol.* **2007**, *374* (5), 1251−1269.
(33) Wender, P. A.; Mitchell, D. J.; Pattabiraman, K.; Pelkey, E. T.; Steinman, L.; Rothbard, J. B. *Proc. Natl. Acad. Sci. U. S. A.* **2000**, *97* (24), 13003−13008.
(34) Wiegand, I.; Hilpert, K.; Hancock, R. E. W. *Nat. Protoc.* **2008**, *3* (2), 163−175.
(35) Phillips, J. C.; Braun, R.; Wang, W.; Gumbart, J.; Tajkhorshid, E.; Villa, E.; Chipot, C.; Skeel, R. D.; Kale, L.; Schulten, K. *J. Comput. Chem.* **2005**, *26* (16), 1781−1802.
(36) Ivanov, I.; Vemparala, S.; Pophristic, V.; Kuroda, K.; DeGrado, W. F.; McCammon, J. A.; Klein, M. L. *J. Am. Chem. Soc.* **2006**, *128* (6), 1778−1779.
(37) Klauda, J. B.; Venable, R. M.; Freites, J. A.; O'Connor, J. W.; Tobias, D. J.; Mondragon-Ramirez, C.; Vorobyov, I.; MacKerell, A. D.; Pastor, R. W. *J. Phys. Chem. B* **2010**, *114* (23), 7830−7843.
(38) Jorgensen, W. L.; Chandrasekhar, J.; Madura, J. D.; Impey, R. W.; Klein, M. L. *J. Chem. Phys.* **1983**, *79* (2), 926−935.
(39) Palermo, E.; Kuroda, K. *Biomacromolecules* **2009**, *10* (6), 1416−1428.
(40) Thomas, J. L.; Chung, J.; Gross, D.; Tirrell, D. *Abstr. Pap. Am. Chem. Soc.* **1995**, *210*, 56-POLY.
(41) Thomas, J. L.; You, H.; Tirrell, D. A. *J. Am. Chem. Soc.* **1995**, *117* (10), 2949−2950.
(42) Geurts, J. M.; Gottgens, C. M.; Van Graefschepe, M. A. I.; Welland, R. W. A.; Van Es, J. J. G.; German, A. L. *J. Appl. Polym. Sci.* **2001**, *80* (9), 1401−1415.
(43) He, L. H.; Read, E. S.; Armes, S. P.; Adams, D. J. *Macromolecules* **2007**, *40* (13), 4429−4438.
(44) Zhang, Y. F.; Lu, H.; Lin, Y.; Cheng, J. J. *Macromolecules* **2011**, *44* (17), 6641−6644.
(45) Adams, M. D.; Chan, E. R.; Molyneaux, N. D.; Bonomo, R. A. *Antimicrob. Agents Chemother.* **2010**, *54* (9), 3569−3577.
(46) Boles, B. R.; Thoendel, M.; Roth, A. J.; Horswill, A. R. *PloS One* **2010**, *5* (4), e10146.
(47) Sovadinova, I.; Palermo, E. F.; Huang, R.; Thoma, L. M.; Kuroda, K. *Biomacromolecules* **2011**, *12* (1), 260−268.
(48) Wilkinson, S. G. *Microbial Lipids*; Academic Press: London, 1988; Vol. *1*.
(49) Mondal, J.; Zhu, X.; Cui, Q. A.; Yethiraj, A. *J. Phys. Chem. B* **2010**, *114* (42), 13585−13592.
(50) Leontiadou, H.; Mark, A. E.; Marrink, S. J. *J. Am. Chem. Soc.* **2006**, *128* (37), 12156−12161.